

Upper limit on the prompt muon flux derived from the LVD underground experiment

M. Aglietta,¹⁶ B. Alpat,¹³ E. D. Alyea,⁷ P. Antonioli,¹ G. Badino,¹⁶ G. Bari,¹ M. Basile,¹ V. S. Berezinsky,¹⁰ F. Bersani,¹ M. Bertaina,¹⁶ R. Bertoni,¹⁶ G. Bonoli,¹ A. Bosco,² G. Bruni,¹ G. Cara Romeo,¹ C. Castagnoli,¹⁶ A. Castellina,¹⁶ A. Chiavassa,¹⁶ J. A. Chinellato,³ L. Cifarelli,^{1,*} F. Cindolo,¹ G. Conforto,¹⁷ A. Contin,¹ V. L. Dadykin,¹⁰ A. De Silva,² M. Deutsch,⁸ P. Dominici,¹⁷ L. G. Dos Santos,³ L. Emaldi,¹ R. I. Enikeev,¹⁰ F. L. Fabbri,⁴ W. Fulgione,¹⁶ P. Galeotti,¹⁶ C. Ghetti,¹ P. Ghia,¹⁶ P. Giusti,¹ R. Granella,¹⁶ F. Grianti,¹ G. Guidi,¹⁷ E. S. Hafen,⁸ P. Haridas,⁸ G. Iacobucci,¹ N. Inoue,¹⁴ E. Kemp,³ F. F. Khalchukov,¹⁰ E. V. Korolkova,¹⁰ P. V. Korchaguin,¹⁰ V. B. Korchaguin,¹⁰ V. A. Kudryavtsev,^{10,**} K. Lau,⁶ M. Luvisetto,¹ G. Maccarone,⁴ A. S. Malguin,¹⁰ R. Mantovani,¹⁷ T. Massam,¹ B. Mayes,⁶ A. Megna,¹⁷ C. Melagrana,¹⁶ N. Mengotti Silva,³ C. Morello,¹⁶ J. Moromisato,⁹ R. Nania,¹ G. Navarra,¹⁶ L. Panaro,¹⁶ L. Periale,¹⁶ A. Pesci,¹ P. Picchi,¹⁶ L. Pinsky,⁶ I. A. Pless,⁸ J. Pyrlík,⁶ V. G. Rzasny,¹⁰ O. G. Ryazhskaya,¹⁰ O. Saavedra,¹⁶ K. Saitoh,¹⁵ S. Santini,¹⁷ G. Sartorelli,¹ M. Selvi,¹ N. Taborgna,⁵ V. P. Talochkin,¹⁰ J. Tang,⁸ G. C. Trincherro,¹⁶ S. Tsuji,¹¹ A. Turtelli,³ I. Uman,¹³ P. Vallania,¹⁶ G. Van Buren,⁸ S. Vernetto,¹⁶ F. Vetrano,¹⁷ C. Vigorito,¹⁶ E. von Goeler,⁹ L. Votano,⁴ T. Wada,¹¹ R. Weinstein,⁶ M. Widgoff,² V. F. Yakushev,¹⁰ I. Yamamoto,¹² G. T. Zatsepin,¹⁰ and A. Zichichi¹

(The LVD Collaboration)

¹University of Bologna and INFN-Bologna, Bologna, Italy 40126

²Brown University, Providence, Rhode Island 02912

³University of Campinas, Campinas, Brazil 13081

⁴INFN-LNF, Frascati, Italy 00044

⁵INFN-LNGS, Assergi, Italy 67010

⁶University of Houston, Houston, Texas 77004

⁷Indiana University, Bloomington, Indiana 47405

⁸Massachusetts Institute of Technology, Cambridge, Massachusetts 02139

⁹Northeastern University, Boston, Massachusetts 02115

¹⁰Institute for Nuclear Research, Russian Academy of Sciences, Moscow, Russia 117312

¹¹Okayama University, Okayama, Japan 700-85301

¹²Okayama University of Science, Okayama, Japan 700-85301

¹³University of Perugia and INFN-Perugia, Perugia, Italy 06100

¹⁴Saitama University, Saitama, Japan 338-8570

¹⁵Ashikaga Institute of Technology, Ashikaga, Japan

¹⁶Institute of Cosmo-Geophysics, CNR, Torino, University of Torino and INFN-Torino, Turin, Italy 10100

¹⁷University of Urbino and INFN-Firenze, Urbino, Italy 61029

(Received 3 June 1998; revised manuscript received 16 March 1999; published 5 November 1999)

We present the analysis of the muon events with all muon multiplicities collected during 21804 h of operation of the first LVD tower. The measured depth-angular distribution of muon intensities has been used to obtain the normalization factor A the power index γ of the primary all-nucleon spectrum, and the ratio R_c of the prompt muon flux to that of π mesons—the main parameters which determine the spectrum of cosmic ray muons at the sea level. The values of $\gamma = 2.77 \pm 0.05$ (68% C.L.) and $R_c < 2.0 \times 10^{-3}$ (95% C.L.) have been obtained. The upper limit to the prompt muon flux favors the models of charm production based on QGSM and the dual parton model. [S0556-2821(99)03917-X]

PACS number(s): 13.85.Tp, 96.40.Tv

I. INTRODUCTION

The depth-angular distribution of muon intensity measured in an underground experiment is closely related to the muon energy spectrum at the surface. Assuming the muon survival probabilities are well known for every depth and every muon energy at the surface, the analysis of the mea-

sured depth-zenith angle distribution of intensity allows us to evaluate the parameters of the muon spectrum at sea level, i.e., the normalization constant, the power index of the primary all-nucleon spectrum, γ , and the prompt muon flux from the decay of charmed particles produced together with pions and kaons in the high-energy hadron-nucleus interactions.

Among these characteristics the value of the prompt muon flux attracts particular interest. It can be evaluated from the zenith-angle distributions of muon intensities, measured at various muon energies or various depths. The fraction of prompt muons cannot be estimated from the muon energy spectrum or depth-intensity curve measured at one zenith angle because the same effect can be produced either by the

*Present address: University of Salerno and INFN-Salerno, Salerno, Italy.

**Present address: University of Sheffield, Sheffield, United Kingdom.

prompt muons, or the decrease of γ , or both.

The charmed particles are produced together with pions and kaons in the collisions of primary cosmic rays with air nuclei. They have such short live times that they decay immediately (if their energy is less than 1000 TeV) into muons and other particles. Thus, for them there is no competition between interaction and decay, and the prompt muon energy spectrum has almost the same slope as the primary spectrum. Because of the rise of the charm production cross section in the energy range 100–1000 TeV, the power index of the prompt muon spectrum, γ_c , can be a little lower than γ . However, possible scaling violation in the fragmentation region can increase the value of γ_c . Because of the absence of the competition between interaction and decay of charmed particles the zenith-angle distribution of prompt muons is almost flat, compared with the $\sec \theta$ distribution of the conventional muons (from the decay of pions and kaons). This allows us to estimate the fraction of prompt muons by analyzing the zenith-angle distribution of muon intensities.

Numerous calculations of the prompt muon flux were done (see, for example, [1–8]). Different models give the prompt muon fluxes which vary by 2 orders of magnitude. This is due to the uncertainties in the charm production cross section, σ_c , x distribution of charmed particles ($x = E_c/E_0$), produced in pA collisions, and the branching ratio of charmed particle decay into muons. The most uncertain parameter, that results in the large dispersion of the predicted prompt muon flux, is the x distribution of produced charmed particles in the fragmentation region, important for the charm-produced cosmic-ray muons. This distribution at high energies cannot be measured precisely at accelerators which give the information only about small x . Thus, to check the models of the charm production, the experiments with cosmic-ray muons at high energies are useful.

The search for the prompt muon flux was done with several detectors located at the surface and underground (see, for example, [9–12]). In practice, it is convenient to express the prompt muon flux in terms of the ratio, R_c , of prompt muon flux to that of pions at vertical. Since the slope of the prompt muon spectrum is close to that of pion spectrum, the ratio R_c is almost constant for all muon energies available in the existing experiments. The experimental data, collected up to now, show a large variation of R_c (from 0 to 4×10^{-3}).

In a previous paper [13] we have presented our measurement of the single muon “depth-vertical intensity” curve and the evaluation of the power index of the meson spectrum in the atmosphere using the “depth-vertical intensity” relation for single muons. Here we present the analysis of all muon sample which include the muon events with all multiplicities. The muon survival probabilities, used to obtain the value of γ in [13], have been presented in [14]. They have been calculated using the muon interaction cross sections from [15–17]. After the publication of these results, new calculation of the cross section of muon bremsstrahlung and of the corrections to the knock-on electron production cross section have been done [18]. In the present analysis we have taken into account the corrections proposed in [18] and we have estimated the uncertainties of γ due to the uncertainties of the cross sections used to simulate the muon transport

through the rock. In this paper we present a more detailed evaluation of the characteristics of the muon spectrum at the sea level, including the ratio of the prompt muon flux to that of pions, using the depth-zenith angle distributions of muon intensities ($I_\mu(x, \theta)$) measured with LVD in the underground Gran Sasso Laboratory. The analysis is based on an increased statistics comparing with the previous publications. The “depth-vertical intensity” relation for all muon sample and its analysis are presented in a separate paper [19].

In Sec. II the detector and the procedure of data processing are briefly described. In Sec. III the results of the analysis of the muon intensity distribution ($I_\mu(x, \theta)$) are presented. In Sec. IV we discuss our results in comparison with the data of other experiments and theoretical expectations. Section V contains the conclusions.

II. LVD AND DATA PROCESSING

The LVD (Large Volume Detector) experiment is located in the underground Gran Sasso Laboratory at a minimal depth of about 3000 hg/cm². The LVD will consist of 5 towers. The 1st tower has been running since June 1992, and the 2nd one since June 1994. The data presented here were collected with the 1st LVD tower during 21804 h of live time.

The 1st LVD tower contains 38 identical modules [20]. Each module consists of 8 scintillation counters and 4 layers of limited streamer tubes (tracking detector) attached to the bottom and to one vertical side of the supporting structure. A detailed description of the detector was given in [20]. One LVD tower has the dimensions of $13 \times 6.3 \times 12$ m³.

The LVD measures the atmospheric muon intensities from 3000 hg/cm² to more than 12000 hg/cm² (which correspond to the median muon energies at the sea level from 1.5 TeV to 40 TeV) at the zenith angles from 0° to 90° (on the average, the larger depths correspond to higher zenith angles).

We have used in the analysis the muon events with all multiplicities, as well as the sample of single muons. Our basic results have been obtained with all muon sample. This sample contains about 2 million reconstructed muon tracks.

The acceptances for each angular bin have been calculated using the simulation of muons passing through LVD taking into account muon interactions with the detector materials and the detector response. The acceptances for both single and multiple muons were assumed to be the same.

As a result of the data processing the angular distribution of the number of detected muons $N_\mu(\phi, \cos \theta)$ has been obtained. The angular bin width $1^\circ \times 0.01$ has been used. The analysis refers to the angular bins for which the efficiency of the muon detection and track reconstruction is greater than 0.03. We have excluded from the analysis the angular bins with a large variation of depth.

The measured $N_\mu(\phi, \cos \theta)$ distribution has been converted to the depth-angular distribution of muon intensities, $I_\mu(x, \cos \theta)$, using the formula

$$I_\mu(x_m, \cos \theta_i) = \frac{\sum_j N_\mu(x_m(\phi_j), \cos \theta_i)}{\sum_j [A[x_m(\phi_j), \cos \theta_i] \epsilon[x_m(\phi_j), \cos \theta_i] \cdot \Omega_{ij} \cdot T]}, \quad (1)$$

where the summing up has been done over all angles ϕ_j contributing to the depth x_m ; $A(x_m(\phi_j), \cos \theta_i)$ is the cross section of the detector in the plane perpendicular to the muon track at the angles $(\phi_j, \cos \theta_i)$; $\epsilon(x_m(\phi_j), \cos \theta_i)$ is the efficiency of muon detection and reconstruction; Ω_{ij} is the solid angle for the angular bin, and T is the live time. We have chosen the depth bin width increasing with the depth to have comparable statistics at all depth bins from 3 to 10 km w.e. Thus, the depth bin width increases from about 100 m w.e. at 3000 m w.e. to more than 500 m w.e. at about 10000 m w.e. The muon intensities have been converted to the middle points of the depth bins taking into account the predicted depth-intensity relations for different zenith angles (we have used the parameters of the muon spectrum at sea level which fit well the ‘‘depth-vertical muon intensity’’ relation measured by LVD [13]). The angular bin width has been taken equal to $\Delta(\cos \theta)=0.025$. The conversion to the middle points of the angular bins has been done according to the predicted angular dependence for muons from pion and kaon decay. However, due to the small angular bins this conversion does not change angular distributions.

III. ANALYSIS OF THE DEPTH-ZENITH ANGLE DISTRIBUTION OF MUON INTENSITY MEASURED BY LVD

The data analysis has included the procedure of fitting of the measured depth-zenith angle distribution of muon intensity with the distributions calculated using the known muon survival probabilities (see [13,14], and references therein) modified for a new muon bremsstrahlung cross section [18] and muon spectrum at sea level with three free parameters: normalization constant, A , power index of primary all-nucleon spectrum, γ , and the ratio of prompt muons to pions, R_c . The depth-angular distributions of muon intensity have been calculated using the equation

$$I_\mu(x, \cos \theta) = \int_0^\infty P(E_{\mu 0}, x) \frac{dI_{\mu 0}(E_{\mu 0}, \cos \theta)}{dE_{\mu 0}} dE_{\mu 0}, \quad (2)$$

where $P(E_{\mu 0}, x)$ is the probability for muon with an initial energy $E_{\mu 0}$ at sea level to survive at the depth x in Gran Sasso rock, and $dI_{\mu 0}(E_{\mu 0}, \cos \theta)/dE_{\mu 0}$ is the muon spectrum at sea level which has been taken according to [21]

$$\frac{dI_{\mu 0}(E_{\mu 0}, \cos \theta)}{dE_{\mu 0}} = A \times 0.14 \times E_{\mu 0}^{-\gamma} \left(\frac{1}{1 + \frac{1.1 E_{\mu 0} \cos \theta^*}{115 \text{ GeV}}} + \frac{0.054}{1 + \frac{1.1 E_{\mu 0} \cos \theta^*}{850 \text{ GeV}}} + R_c \right), \quad (3)$$

where the values of $\cos \theta$ have been substituted by $\cos \theta^*$ which have been taken from either [22] or a simple consideration of the curvature of the Earth atmosphere. In a search for a small contribution of prompt muons it is necessary to know precisely the angular dependence of conventional (from pion and kaon decay) muon intensity at all energies of interest. In [22] $\cos \theta^* = E_{\pi, K}^{cr}(\cos \theta=1)/E_{\pi, K}^{cr}(\cos \theta)$, where $E_{\pi, K}^{cr}$ are the critical energies of pions and kaons. $\cos \theta^*$ can be understood also as the cosine of zenith angle of muon direction at the height of muon production. The height of muon production increases from 17 km at $\cos \theta=1$ to about 32 km at $\cos \theta=0$. We have found that the values of $\cos \theta^*$ depend on the model of the atmosphere in the range of $\cos \theta=0-0.3$. In Fig. 1 we present the predicted angular dependences of conventional muon intensities at the energy of 10 TeV. As can be seen, all curves almost coincide at $\cos \theta=0.3-1$. However, there is a large spread of functions at $\cos \theta=0-0.3$. The calculations using Eq. (3) with $\cos \theta^*$ from [22] (upper solid curve) or the treatment of the Earth curvature with a muon production height of 32 km (dash-dotted curve), as well as the results of [23] (dashed curve) give quite similar results at all $\cos \theta$, while the original calculations of [22,24] (lower solid curve) and the treatment of the Earth curvature with a muon production height of 17 km (dotted curve) are far below or above other curves at small $\cos \theta$. To be independent of the model we have restricted the range of $\cos \theta$ used in the analysis to 0.3–1. This increases the statistical error of the results decreasing at the same time

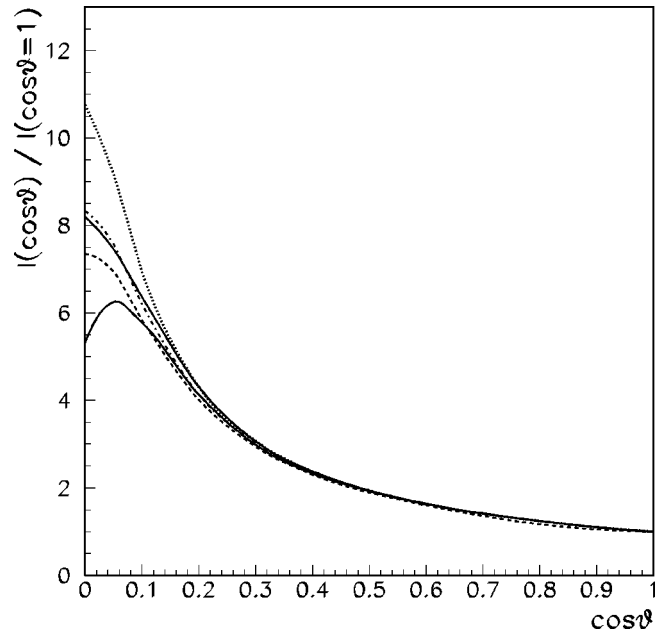


FIG. 1. Ratio of muon intensity at $\cos \theta$ to that at $\cos \theta=1$ for 10 TeV muons at sea level versus cosine of zenith angle $\cos \theta$ calculated using different formulas; dotted curve—Eq. (3) with $\cos \theta^*$ from Earth curvature with scale height of 17 km; dash-dotted curve—Eq. (3) with $\cos \theta^*$ from Earth curvature with scale height of 32 km; upper solid curve—Eq. (3) with $\cos \theta^*$ from [21]; dashed curve—calculations of [22]; lower solid curve—original formula from [21,23].

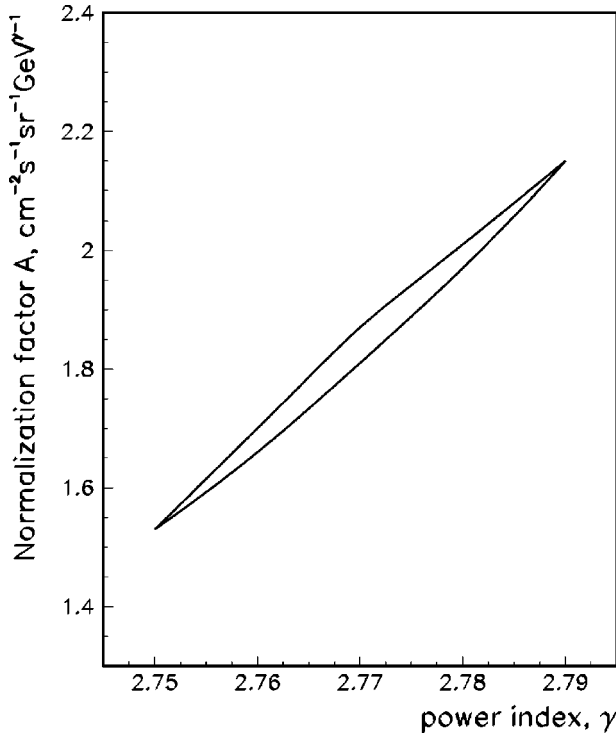


FIG. 2. Contour plot of allowed region in $A - \gamma$ plane showing strong correlation between the parameters.

the systematical uncertainty related to model used. This also reduces the sensitivity of the experiment to small values of R_c . We note that the uncertainties in the rock thickness and rock density are high enough at small $\cos \theta$. Moreover, large derivative of the column density with angle together with muon scattering effect lead to the high uncertainties of the muon flux. This also justifies our decision to restrict the range of zenith angles used in the analysis.

We have added to the original formula of [21] the term R_c , which is the ratio of prompt muons to pions. Here it has been assumed that the power index of the prompt muon spectrum is equal to that of primary spectrum. Really, due to rapid rise of charm production cross section and the possible scaling violation in the fragmentation region, the prompt muon spectrum may have the power index, γ_c , different from γ . But the value of γ_c depends on the model of charm production. To be independent of the models we have used at the first approximation the assumption: $\gamma_c = \gamma$. The full formula has been multiplied by the additional normalization constant A which has been considered as a free parameter together with γ and R_c .

As a result of the fitting procedure we have obtained the values of the free parameters: $A = 1.84 \pm 0.31$, $\gamma = 2.77 \pm 0.02$ and the upper limit on $R_c \leq 2 \times 10^{-3}$. Here and hereafter we present the errors at 68% confidence level (C.L.) and the upper limits at 95% C.L. The value of χ^2 is equal to 316.7 for 330 degrees of freedom. The estimates of the parameters A and γ are strongly correlated. The larger the value of γ is, the larger the normalization factor A should be. Figure 2 shows the contour plot of allowed region in $A - \gamma$ -plane. The dependence of χ^2 on R_c is presented in Fig.

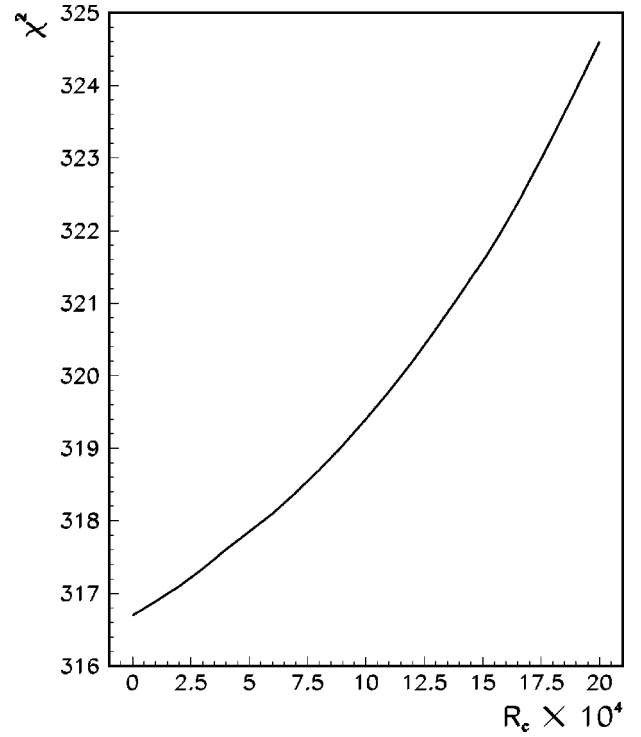


FIG. 3. Dependence of χ^2 on the ratio of prompt muon flux to that of pions.

3 which was used to obtain an upper limit on R_c . The errors of the parameters include both statistical and systematic uncertainties. The latter one takes into account the possible uncertainties in the depth and local density, but does not take into account the uncertainty in the cross sections used to simulate the muon transport through the rock. If we add the uncertainty in the muon interaction cross sections, the error of γ will increase from 0.02 to 0.05 (for the discussion about the uncertainty due to different cross sections see [25]). This uncertainty, however, does not influence the upper limit on R_c . We note that the energy in Eq. (3) is expressed in GeV and the intensity is expressed in $\text{cm}^{-2} \text{s}^{-1} \text{sr}^{-1}$. If we restrict our analysis to the depth range 5–10 km w.e., we obtain the following values of parameters: $A = 1.6_{-0.6}^{+0.8}$, $\gamma = 2.76 \pm 0.06$ and $R_c \leq 3 \times 10^{-3}$.

The angular distributions of muon intensities for depth ranges of interest are presented in Fig. 4 together with calculations with $R_c = 0$ (best fit, solid curve) and $R_c = 2 \times 10^{-3}$ (upper limit, dashed curve). The normalizations of both calculations have been done independently using the fitting procedure. The data at all zenith angles are shown but the analysis was restricted to the range $0.3 < \cos \theta < 1$. The error bars show both statistical and systematic uncertainties. The calculated distributions have been obtained using Eq. (3) and the values of $\cos \theta^*$ from [22]. As can be seen from Fig. 4, there is no evident increase of the deflection of the data points from the best fit predictions ($R_c = 0$) with the increase of depth at large $\cos \theta$ as it should be if the significant prompt muon flux is present. The deepest depth bin is the exception. However, due to small statistics, the data at very large depth do not affect much the total value of χ^2 .

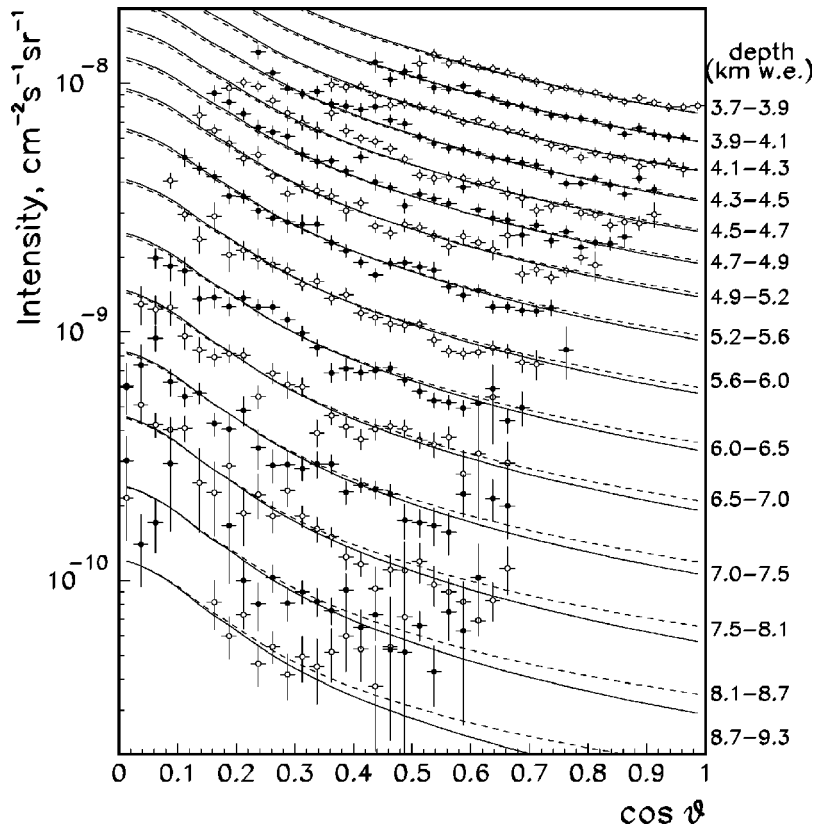


FIG. 4. The dependence of the muon intensity on the zenith angle for the depth bins of most interest in the analysis and for all zenith angles. The data have been converted to the middle points of depth and angular bins. Solid curve—calculation with $\gamma=2.77$ and $R_c=0$ [best fit to the LVD data in the whole depth range; see Eq. (3)]; dashed curve—calculation with $\gamma=2.77$ and $R_c=2 \times 10^{-3}$ (LVD upper limit). The absolute normalization of both sets of calculations has been done independently using the fitting procedure. The error bars include both statistical and systematic uncertainties.

If the formula from [24] is used for the muon spectrum at sea level instead of Eq. (3), the best fit values of γ will be decreased by 0.04–0.05 and will be in agreement with the previously published values for single muons [13,14] analyzed using the formula from [24]. This difference, being comparable with our total error, is due to the factor which is present in the formula from [24] and takes into account the rise of hadron-nucleus cross section at high energies. This factor appears in the calculation [24] if the rise of the total hadron-nucleus cross section with energy is due to the rise of the differential cross section in the central region, while the scaling is conserved in the fragmentation region. This factor makes the muon energy spectrum steeper and the difference in the power index of muon spectrum is about 0.04–0.05.

Similar analysis performed for single muons shows no evidence for prompt muon flux, too. We found the same values of power index and upper limit to the prompt muon flux, while the absolute intensity is 10% smaller.

IV. DISCUSSION

From the analysis of the depth-angular and depth distributions of muon intensities measured by LVD the following estimates of the parameters of the muon spectrum at the sea level have been obtained: $A = 1.84 \pm 0.31$, $\gamma = 2.77 \pm 0.02$ (68% C.L.), $R_c \leq 2 \times 10^{-3}$ (95% C.L.). The errors include both statistical and systematic errors with the systematic error dominating. The systematic error takes into account the possible uncertainties in the depth and local density, which have been estimated from the difference between the measured and predicted intensities for all angular and depth bins. The

uncertainties of rock thickness and local density both result in the uncertainty of the column density and, hence, in the uncertainty of the muon flux. The distribution of fractional differences between measured and predicted intensities has been found to be close to Gaussian with a standard deviation of about 0.04. This value has been assumed as a systematic error of muon intensity due to the column density uncertainty. This value is equivalent to the column density error of about 1% at a depth of 3 km w.e. It is obvious that the systematic error is more important at small depth where the statistics is high and statistical error is negligibly small. An additional systematic error due to the uncertainties of the cross sections of muon interactions used to simulate the muon survival probabilities should be included. According to the discussion in [25] we estimate the total uncertainty in γ as 0.05 and in A as 0.5. The uncertainty in the cross sections, however, does not affect the upper limit to R_c . To check this we have fitted LVD data with the intensities calculated with muon bremsstrahlung cross section from [15] and obtained the following results: $A = 1.86 \pm 0.32$, $\gamma = 2.78 \pm 0.02$ (68% C.L.), $R_c \leq 2 \times 10^{-3}$ (95% C.L.). The muon bremsstrahlung cross section from [15] is a little smaller than that from [18]. This makes the muon “depth-intensity” curve (with fixed A , γ and R_c) flatter. This is compensated in the data analysis by the increase of γ . But the shape of the calculated angular distribution of muon intensities at any fixed depth, used to extract the value of R_c , is not changed and, hence, the limit on ratio of prompt muon flux to that of pions remains unchanged. However, the absolute value of prompt muon flux (or its limit) varies with the muon cross sections used since

the flux depends also on normalization constant, A , and power index, γ [see Eq. (3)].

The value of γ obtained with LVD data is in reasonable agreement with the results of many other surface and underground experiments (see, for example, [12,26–31]). However, the results obtained in the experiments which used the indirect method of the measurement of the muon spectrum, in particular, the measurement of the depth-intensity curve, are strongly affected by the muon interaction cross sections and the algorithm applied to calculate the muon intensities. We have used the most accurate cross sections, known at present, and the algorithm which allows us to calculate the muon intensities with an accuracy of 1% for a given set of muon interaction cross sections and for homogeneous medium. The algorithm can influence strongly the calculated muon intensities and, then, the final results (for a discussion see, for example [25]). Thus, the observed agreement (or disagreement) in the value of γ does not mean the agreement (or disagreement) in the data themselves.

The conservative upper limit to the fraction of prompt muons, obtained with the LVD data ($R_c < 2 \times 10^{-3}$), even in the simple assumption that the power index of the prompt muon spectrum, γ_c , is equal to that of primaries, γ , rules out many models of the prompt muon production, which predict a fraction of prompt muons more than 2×10^{-3} . To make this conclusion more reliable we have carried out the analysis of the depth-angular distribution of muon intensity using the prompt muon spectra predicted by different models (without a constant term R_c). We conclude that the LVD data contradict the predictions of model 1 [1], model II [3] and model A [5]. The predictions of the model 3 [1], model I [3], models B, C [5], recombination quark-parton model (RQPM) [6] and model by [4] are comparable with the LVD upper limit, and these models cannot be ruled out. At the same time the LVD result favors the models of charm production based on QGSM (see, for example, [6]) and the dual parton model [7], which predict low prompt muon flux.

The upper limit (95% C.L.) obtained with the LVD data is lower than the value of R_c found in the MSU experiment

[$R_c = (2.6 \pm 0.8) \times 10^{-3}$ at $E_{\mu 0} = 5$ TeV [12]]. The LVD upper limit does not contradict the values of prompt muon flux, obtained in Baksan [11] and Kolar Gold Field (KGF) [9] underground experiments. Our result agrees with that of NUSEX [10] which did not reveal any deviation from the angular distribution expected for conventional muons.

We point out that the LVD sensitivity to the prompt muon flux is restricted mainly by the systematic uncertainties connected with the uncertainties of the slant depth and local density fluctuations and the differences in the theoretical shape of the muon underground intensities.

V. CONCLUSIONS

The analysis of the depth-angular distribution of muon intensity measured by LVD in the depth range 3000–10000 hg/cm² has been done. The parameters of the muon energy spectrum at the sea level have been obtained [see Eq. (3)]: $A = 1.8 \pm 0.5$, $\gamma = 2.77 \pm 0.05$ and $R_c < 2 \times 10^{-3}$ (95% C.L.). The errors include both statistical and systematic uncertainties. The upper limit to the fraction of prompt muons, R_c , favors the models of charm production based on QGSM [6] and the dual parton model [7], and it rules out several models which predict a high prompt muon flux. Similar analysis performed for single muon events revealed the same values of power index and upper limit to the fraction of prompt muons, while the normalization constant is 10% smaller.

ACKNOWLEDGMENTS

We wish to thank the staff of the Gran Sasso Laboratory for their aid and collaboration. This work is supported by the Italian Institute for Nuclear Physics (INFN) and in part by the Italian Ministry of University and Scientific-Technological Research (MURST), the Russian Ministry of Science and Technologies, the Russian Foundation of Basic Research (grant 96-02-19007), the U.S. Department of Energy, the U.S. National Science Foundation, the State of Texas under its TATRP program, and Brown University.

-
- [1] J. W. Elbert, T. K. Gaisser, and T. Stanev, in *DUMAND-80*, Proceedings of the 1980 Symposium, Honolulu, edited by V. J. Stenger (Hawaii DUMAND Center, Honolulu, 1981), Vol. 2, p. 222.
- [2] C. Castagnoli *et al.*, *Nuovo Cimento A* **82**, 78 (1984).
- [3] H. Inazawa, K. Kobayakawa, and T. Kitamura, *Nuovo Cimento C* **9**, 382 (1986).
- [4] L. V. Volkova *et al.*, *Nuovo Cimento C* **10**, 465 (1987).
- [5] E. Zas, F. Halzen, and R. A. Vazquez, *Astropart. Phys.* **1**, 297 (1993).
- [6] E. V. Bugaev *et al.*, in *Proceedings of the RIKEN International Workshop on Electromagnetic and Nuclear Cascade Phenomena in High and Extremely High Energies*, Tokyo, Japan, 1993, edited by M. Ishihara and A. Misaki (RIKEN, Tokyo, 1994), p. 264.
- [7] G. Battistoni *et al.*, in *Proceedings of the 24th International Cosmic Ray Conference*, Rome, Italy, 1995 (Arti Grafiche Editoriali, Urbino, 1995), Vol. 1, p. 532.
- [8] M. Thunman, G. Ingelman, and P. Gondolo, *Astropart. Phys.* **5**, 309 (1996).
- [9] M. R. Krishnaswamai *et al.*, in *Proceedings of the 18th International Cosmic Ray Conference*, Bangalore, India, 1983, edited by N. Durgaprasad *et al.* (TIFR, Bombay, 1983), Vol. 11, p. 450.
- [10] G. Battistoni *et al.*, in *Proceedings of the 20th International Cosmic Ray Conference*, Moscow, USSR, 1987, edited by V. A. Kozyarivsky *et al.* (Nauka, Moscow, 1987), Vol. 9, p. 195.
- [11] Yu. M. Andreyev *et al.*, in *Proceedings of the 21st International Cosmic Ray Conference*, Adelaide, Australia, 1990, edited by R. J. Protheroe (Graphic Services, Northfield, South Australia, 1990), Vol. 9, p. 301.
- [12] N. P. Il'ina *et al.*, in *Proceedings of the 24th International*

- Cosmic Ray Conference* [7], Vol. 1, p. 524.
- [13] LVD Collaboration, M. Aglietta *et al.*, *Astropart. Phys.* **3**, 311 (1995).
- [14] LVD Collaboration, M. Aglietta *et al.*, in *Proceedings of the 24th International Cosmic Ray Conference* [7], Vol. 1, p. 557.
- [15] L. B. Bezrukov and E. V. Bugaev, in *Proceedings of the 17th International Cosmic Ray Conference*, Paris, France, 1981 (Centre d'Etudes Nucleaires, Saclay, 1981), Vol. 7, p. 102.
- [16] L. B. Bezrukov and E. V. Bugaev, in *Proceedings of the 17th International Cosmic Ray Conference* [15], Vol. 7, p. 90.
- [17] R. P. Kokoulin and A. A. Petrukhin, in *Proceedings of the 12th International Cosmic Ray Conference*, Hobart, Tasmania, 1971, edited by A. G. Fenton and K. B. Fenton (University of Tasmania Press, Hobart, 1971), Vol. 6, p. 2436.
- [18] S. R. Kelner, R. P. Kokoulin, and A. A. Petrukhin, *Yad. Fiz.* **60**, 657 (1997) [*Phys. At. Nucl.* **60**, 576 (1997)].
- [19] M. Aglietta *et al.*, *Phys. Rev. D* **58**, 092005 (1998).
- [20] M. Aglietta *et al.*, *Astropart. Phys.* **2**, 103 (1994).
- [21] T. K. Gaisser, *Cosmic Rays and Particle Physics* (Cambridge University Press, Cambridge, England, 1990).
- [22] L. V. Volkova, Lebedev Physical Institute Report No. 72 (1969).
- [23] P. Lipari, *Astropart. Phys.* **1**, 195 (1993).
- [24] L. V. Volkova, G. T. Zatsepin, and L. A. Kuzmichev, *Yad. Fiz.* **29**, 1252 (1979) [*Sov. J. Nucl. Phys.* **29**, 645 (1979)].
- [25] P. Antonioli *et al.*, *Astropart. Phys.* **7**, 357 (1997).
- [26] O. C. Allkofer *et al.*, in *Proceedings of the 17th International Cosmic Ray Conference* [15], Vol. 10, p. 321.
- [27] S. Matsuno *et al.*, *Phys. Rev. D* **29**, 1 (1984).
- [28] F. F. Khalchukov *et al.*, in *Proceedings of the 19th International Cosmic Ray Conference*, La Jolla, California, 1985, edited by A. Roberts (Scripps Institute of Oceanography, La Jolla, 1985), Vol. 8, p. 12; R. I. Enikeev *et al.*, *Yad. Fiz.* **47**, 1649 (1988) [*Sov. J. Nucl. Phys.* **47**, 1044 (1988)].
- [29] V. D. Ashitkov *et al.*, in *Proceedings of the 19th International Cosmic Ray Conference* [28], Vol. 8, p. 77.
- [30] G. Battistoni *et al.*, *Nuovo Cimento C* **9**, 196 (1986).
- [31] MACRO Collaboration, M. Ambrosio *et al.*, *Phys. Rev. D* **52**, 3793 (1995).